



The instrumented dynamic perforation test applied to a composite shell

Stephane Pattofatto, Elli Tsitsiris, Han Zhao

► **To cite this version:**

Stephane Pattofatto, Elli Tsitsiris, Han Zhao. The instrumented dynamic perforation test applied to a composite shell. DYMAT 2009, Sep 2009, Bruxelles, Belgium. pp.103-109. hal-00436387

HAL Id: hal-00436387

<https://hal.archives-ouvertes.fr/hal-00436387>

Submitted on 26 Nov 2009

HAL is a multi-disciplinary open access archive for the deposit and dissemination of scientific research documents, whether they are published or not. The documents may come from teaching and research institutions in France or abroad, or from public or private research centers.

L'archive ouverte pluridisciplinaire **HAL**, est destinée au dépôt et à la diffusion de documents scientifiques de niveau recherche, publiés ou non, émanant des établissements d'enseignement et de recherche français ou étrangers, des laboratoires publics ou privés.

The instrumented dynamic perforation test applied to a composite shell

S. Pattofatto, H. Tsitsiris and H. Zhao

LMT-Cachan (ENS Cachan/CNRS/Universite Paris 6/PRES UniverSud Paris) 61 av. du President Wilson, F-94230 Cachan, France

Abstract. Perforation tests are commonly used on composites but give limited results. In this study, a single layer of a thermoplastic woven composite is tested at high velocity (45 m/s) by means of an instrumented perforation test. First, an inversed dynamic perforation tests is performed with a modified Hopkinson bar apparatus. This allows to measure accurately the perforation curve (force vs. displacement). Such a test is supplemented by the analysis of the strain displacement field measured by digital image correlation during the perforation process. This gives relevant information in case of inversed identification of several behavior parameters. This measurement technique allows to take into account the anisotropy of the material or an accurate estimation of the boundary conditions. A new experimental procedure is conducted for both quasi-static and dynamic tests. Results are presented concerning two points: the uncertainty of the measurements and the correction of boundary conditions from optical measurements.

1. INTRODUCTION

Due to their light weight, fibre reinforced composite materials are increasingly used in the automotive industry for environment purposes [1]. The use of composites for structural applications is also of great interest and this leads to the processing of new materials that need to be characterized [2]. We focus on a long fibres composite, fully recyclable, with fast processability that is used in the car industry as the skin part of a sandwich structural material. It is made with long glass fibres and a polypropylene matrix. Such TP-composite is a good candidate for applications in automotive applications because of the common polypropylene matrix. Moreover, it is easy to form in order to design complex parts.

The reinforcement of the TP-composite is a fabric of long glass fibres yarns structured as a balanced weave of commercial Twintex[®]. Twintex[®] is a commingled E-glass and iPP filaments composite that is widely used in multilayers composite parts. The meso-structure of the studied material is therefore intrinsically anisotropic, that is the main property that we focus on. The viscoelasticity induced by the matrix and the damage induced by mechanical loading won't be studied here. The thickness of the shell is 0.8 mm. We also mention that a thin layer of PP is also present on one side of the TP-composite bound for linking the skin to the core material of the sandwich structure.

Classical experiments were performed to identify the macroscopic behavior of the shell material, based on tensile tests with three orientations: 0° and 90° (direction of fibers), and 45°, and the use of digital image correlation as an optical extensometer. It is clear that the description of the behavior with a basic linear orthotropic law is weak but this does not challenge the procedures presented here. The results are condensed as follows:

- (i) in the direction of the fibres, the material is elastic and brittle. Young's moduli can be accurately identified $E_1=10.3$ GPa and $E_2=7.1$ GPa (uncertainty <5 %), and Poisson's ratio are coarsely identified $\nu_{12}=0.26$ and $\nu_{21}=0.18$ (uncertainty <15 %),
- (ii) in the 45° orientation, the response is non linear and exhibits hysteresis. In this case, the secant modulus is used to identify the shear modulus $G_{12}=292$ MPa.

In this way, the paper presented here is focused on one goal: the use of a so-called “perforation test” (that is, before fracture, precisely a flexural bending test) for the characterization of a TP-composite shell. This goal is strongly dependent to the dynamic procedure because at high velocities (strain rate > 100 s⁻¹) tensile tests are not common. On the other hand, perforation experiments conducted on drop weight devices are widely used on composites ([3], and ASTM procedure [4]). Such a test gives an overall result as a force vs. displacement curve that could be enriched. The aim of this work is therefore to provide new procedures for the instrumentation of perforation tests. Of course, this must require an inverse identification procedure [5] because the complexity of the test cannot be described analytically. Thus, two experiments are used: the inversed perforation test based on the Hopkinson bar measurement technique, and the direct perforation test coupled with digital image correlation. We also mention that the bulge test is another analog experiment, widely used for the characterization of metal sheets, also for dynamic strain rates [6]. The work presented here could be applied to such a test.

2. THE INVERSED PERFORATION TEST

The inversed perforation test is an original test based on the Hopkinson bar technique [7,8]. The so-called “perforation test” is considered: a disk of the TP-composite shell (ϕ 48 mm) is held on its circumference and deformed statically or dynamically in its center by a rigid impactor of smaller diameter (ϕ 16mm). The disk specimen is attached to a projectile and launched at around 45 m/s. The perforator is a long Hopkinson bar (marval steel, diam. 16 mm, length 6 m) initially at rest. Such an apparatus allows to measure the histories of perforation force F and displacement U during the whole perforation process with a good accuracy [7]. The same experiments are performed for quasi-static loading as a reference (1 mm/s). Each test was repeated 3 times and tests were also done by reverting the specimen to analyze the effect of the PP layer (called face 2).

All the perforation curves are given in Figure 1. The results are the perforation force and displacement measured at the maximum of the curves, and the perforation energy calculated as the surface underneath the curve. All the results are gathered in table 1.

Table 1. Results of perforation experiments.

| | Perforation force mean [range] (N) | | | Perforation displ. mean [range] (mm) | | | Perforation energy mean [range] (J) | | |
|--------------|---------------------------------------|---------------|------|---|-------------|------|--|---------------|------|
| | Dyn. | St. | Rel. | Dyn. | St. | Rel. | Dyn. | St. | D/S |
| Face 1 | 2300 [600] | 1900 [200] | +20% | 8 [1] | 12 [2] | -33% | 12.1 [1.3] | 10.4 [1.6] | +16% |
| Face 2 | 2700 [100] | 1350 [300] | +99% | 9 [0] | 10 [2] | -10% | 13.6 [3.2] | 7.1 [0.9] | +92% |
| F2/F1 | +17% | -24% | | 13% | -16% | | +12% | -32% | |

It is shown that at 45 m/s there is a significant enhancement of the dynamic perforation force, a decrease of the perforation displacement, and an increase of the energy dissipated. Moreover, we can notice that the results depend strongly on which side of the shell is impacted and in particular the effect of the layer on the parameters is inversed between static and dynamic loadings.

The analysis of post-mortem specimens shows a dramatic difference of the damaged area around the perforated zone, independently of the impacted face. In quasi-static, perforation occurs by macro-cracking and the one or two cracks are located at the interface between yarns (Figure 1). In dynamic, the damaged zone is diffuse, all the yarns under the perforator are broken and videos of the

perforation show the formation of a “debris cloud”. This paper is not willing to explain neither the reason of this enhancement nor the effect of the PP layer.

As regards the perforation curves before fracture, quasi-static and dynamic curves are different: (i) static curve is non-linear due to the geometry of the experiment, and (ii) dynamic curve is roughly bi-linear, due to the interaction of the flexural wave created at the center with the fixing device.

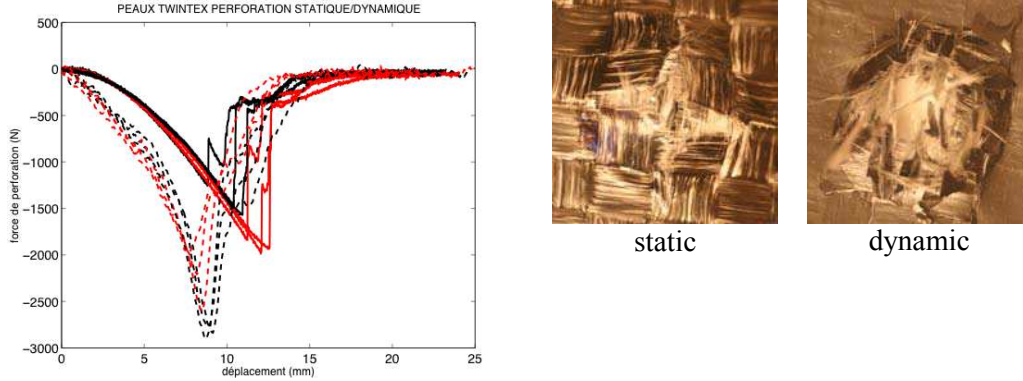


Figure 1. Perforation curves for dynamic (45 m/s) and static experiments. Comparison of fracture zone.

We limit here the analysis of the curves to those three values: force at the peak, displacement at the peak, and energy. In order to get closer to the deformation process during perforation a complementary method is proposed, presented in next section.

3. DIRECT PERFORATION AND DIGITAL IMAGE CORRELATION

A complementary experiment is performed. The goal of this experiment is to provide a measurement of the displacement field that can be used in an inverse identification procedure. A fast camera is used to record the deformation history of the face of the specimen during perforation. A perforator is fixed on a projectile launched at 45 m/s on a specimen held fixed on a framework. Thus, one face of the specimen can be observed by the camera, as depicted in Figure 2a (safe thanks to the use of a mirror placed at 45°). In this case, the perforation curve is no longer measured, that is why this test is said to be complementary to the test presented in previous section. Reference quasi-static perforation tests are done to compare with dynamic experiments. In this case measurement of force, displacement and recording of images can all be performed during the same test.

The parameters of the acquisition of images are the following:

- for quasi-static tests: 1300x1950 at 1 fps (increment of perforation 1 mm),
- for dynamic tests: 256x256 pixels at 30'000 fps (increment of perforation ca. 1.5 mm).

A digital image correlation (DIC) software developed in our laboratory [9], called Correli^{LMT}, is used to calculate the displacement field of the specimen. This program is based on the comparison of two images (the deformed image $g(\underline{x})$ and the image of reference $f(\underline{x})$); each image is discretized in linear quadrangles Q4 elements and the nodal displacement field is computed to minimize a quadratic error η defined as follows:

$$\eta^2 = \iint [\underline{u}(\underline{x}) \cdot \nabla f(\underline{x}) + f(\underline{x}) - g(\underline{x})]^2 d\underline{x} \quad (1)$$

Without going in details into the technique, we mention that Correli^{LMT} allows to compute displacement fields and subsequent strain fields, gives also a field of the residue of the minimization so that the quality of the computation is quantified, and the uncertainty on the displacement due to the algorithm can also be computed on the reference picture. As first insight of the computed results, two displacement fields in direction 1 of the picture are depicted in Figure 2b and 2c, for quasi-static tests performed respectively on the TP-composite shell and for another reference test performed on a ductile A5 aluminium sheet considered as an isotropic material.

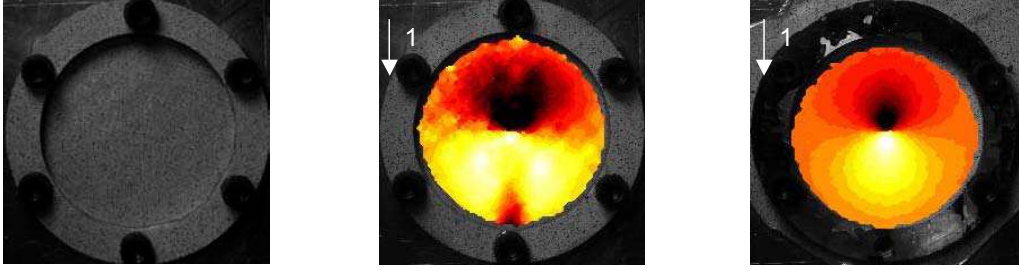


Figure 2. Quasi-static test, (a) raw image of the specimen before the test, (b) 1_displacement field computed for a test on the shell TP-composite, (c) 1_displacement field computed for a test on aluminium sheet.

3.1 Preview of the displacement fields

Results of correlation presented in Figure 2 give a first insight of the improvement of the understanding of the perforation experiment thanks to imaging. The Figure 2c is taken as reference as it corresponds to a case of an isotropic behavior (A5 aluminium sheet, confirmed by a numerical simulation). Figure 2b shows that the anisotropy of the shell TP-composite is well depicted, showing roughly a separation of the isotropic “cockle” picture. This is also visible on the displacement result confirming that this is not due to sliding close to the fixing screws. The accuracy of the correlation procedure allows also to have local information that may be of interest. For example, the analysis of the strain map clearly shows the influence of the heterogeneity of the mesostructure of the material in the deformation process.

Figure 3 shows the evolution of the error field (equation 1) in the case of the dynamic experiment. The error is chosen because it is maximum where the variation of the images is more intense (due to deformation and also variation of light intensity) and therefore it shows clearly the position of the flexural wave propagating from the center to the boundary. The bilinear shape of the perforation curve is as expected due to the interaction of that wave with the boundary.

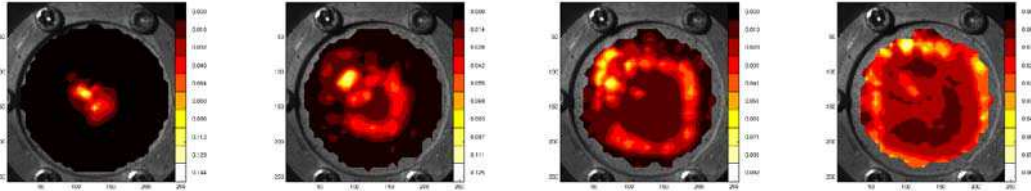


Figure 3. Visualisation of the propagation of the flexural wave during a dynamic perforation test ($dt=35 \mu s$)

3.2 Uncertainty analysis

The authors claim that the knowledge of the displacement field of the shell during a perforation process is a valuable measurement for an improved analysis of such a test. To confirm this point, an uncertainty analysis is conducted as regards two factors: (i) the quality of the images [9], (ii) the quality of the conservation of optical flow during the deformation process, depending on the stationarity of the lighting. The software Correli^{LMT} allows to compute indicators^a on the efficiency of the computation of the displacement field. A given image is submitted numerically to a prescribed displacement \mathbf{u}_{pre} and the estimated displacement \mathbf{u}_{est} is returned. The results are that the raw quality of the images allows the measurement of the displacement with an accuracy of about 3/1000 pixels.

Regarding the conservation of optical flow, it is clear that it cannot be ensured when the shell is lighted by a directional light. This is the case in our tests and the effect of reflections and shades on the calculated displacement field is considered here. Figure 4 shows the value of error for different conditions of lighting. The results show the effect of lighting on the error, directly due to the way the error indicator is calculated (see equation 1). But it does not necessarily imply that the displacement

^a The indicators are: the systematic error $\delta_u = \left\| \langle \mathbf{u}_{est} \rangle - \mathbf{u}_{pre} \right\|$ and the standard uncertainty $\sigma_u = \left\langle \left\| \mathbf{u}_{est} - \langle \mathbf{u}_{est} \rangle \right\|^2 \right\rangle^{1/2}$.

field is wrong. In Figure 4, the strain field is depicted and it is worth to notice the strain field is almost independent of the value of the error in that case. Therefore, when lighting is constant, the time-evolution of the error is a good indicator of the quality of the correlation. The value of the strain induced by this technical noise is about 0.5 %. This value is relatively high and is due (i) to the fact that the variation of lighting induces “shades” on the surface of the material that is not flat due to the weaves, and (ii) to the fact that the correlation was done with a small size of elements of 8 pixels. But in any case, this explains also the difficulty to obtain a good accuracy on the results.

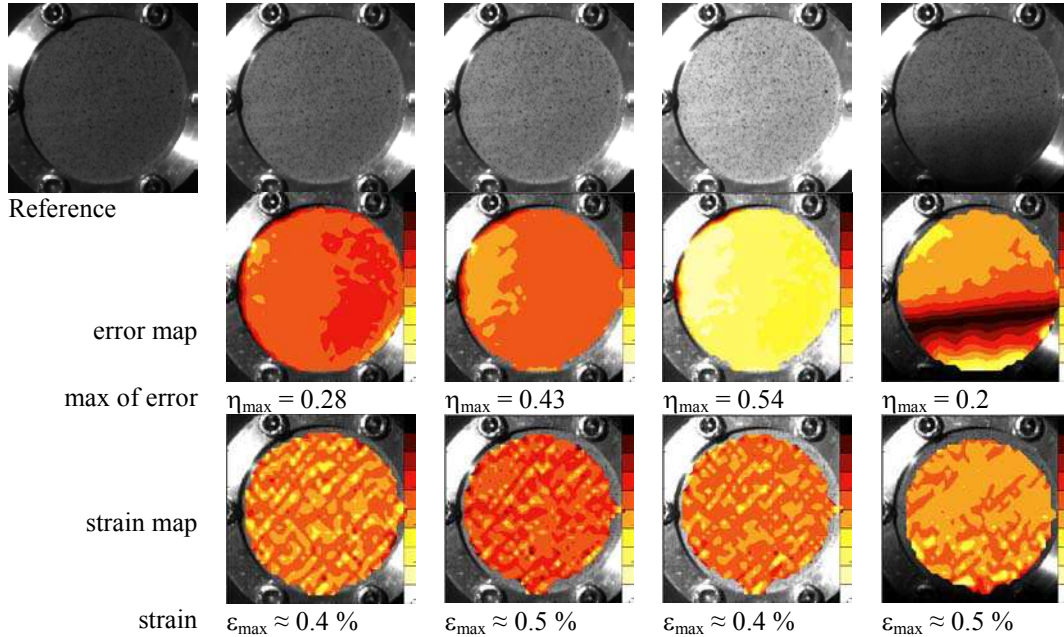


Figure 4. Error (field and maximum value) due to the variation of lighting

3.3 Correction of the boundary conditions

In case of the perforation experiments, the sliding of the specimen at the boundary is one of the critical questions because it is very sensitive and usually it is not measured. The great advantage of the imaging is that displacement at the boundary can be extracted from the displacement field computed by DIC. First we can suppose that close to the framework on which the specimen is fixed, the out-of-plane displacements are negligible. Two results are presented in figure 5. They show the evolution of the displacements U and V along a circle the diameter of which is 90 % of the diameter of the ring on which the specimen is fixed. These displacements here take into account both the out-of-plane displacements, the in-plane due to deformation and the sliding at the boundary. These displacements can then be used as a boundary condition in a FE calculation of the experiment. The results show that without any filtering, the noise on the boundary condition is less than 0.01 mm.

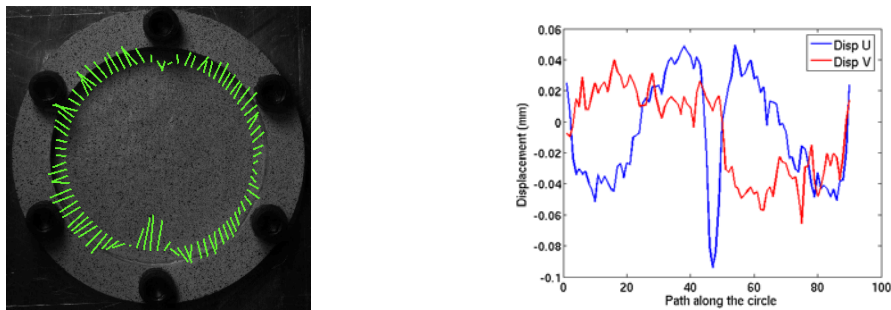


Figure 5. Result of extraction of the displacement along a circle close to the boundary.

4. CONCLUSIONS AND PROSPECTS

Two original experiments were presented, dealing with the dynamic characterization of a TP-composite shell at high impact velocities (45 m/s). The first experiment is a modified Hopkinson bar test applied to perforation. Contrary to a classical drop-weight test, the use of a gas-gun allows to reach high impact velocities and the Hopkinson bar ensures an accurate measurement of force and displacement. The drawback of the test is that the geometry of the specimen is contained by the inner diameter of the barrel of the gas gun. Results are presented. The second experiment is a direct perforation test coupled with a digital image correlation technique. The uncertainty of the measurement is discussed, and in particular the effect of the lighting. The computed displacement fields are analyzed for quasi-static and dynamic experiments. The results show that displacements can be computed with an uncertainty of about 0.1 mm in best conditions. In case of dynamic test, the low resolution implies that the element size is chosen at 8 pixels and the direct consequence is a well-known decrease of the accuracy. For quasi-static case, the displacement field is accurate and a result of extraction along a circle is presented as for the use as boundary condition in a FE computation.

As prospects, we put the stress on the fact that in this paper, out-of-plane displacements (OoPD) are not corrected and influence the measurement of the displacement by digital image correlation. This can be solved and two strategies are for example proposed: either the OoPD are corrected numerically during the inversed identification procedure (this requires an easy calibration during the test), or they can be taken into account directly in the measurement using for example a technique of stereo-correlation. This is the main prospect of this work because such a technique is now available in our lab.

References

- [1] Passaro A., Corvaglia P., Manni O., Barone L., Maffezzoli A. *Polym Compos* (2004), 25, 307–18.
- [2] Alcock A., Cabrera N.O., Barkoula N.-M. and Peijs T., « Low velocity impact performance of recyclable all-polypropylene composites », *Compos. Sc. & Tech.*, (2006), 66, pp 1724–1737.
- [3] Belingardi G., Vadori R., Influence of the laminate thickness in low velocity impact behavior of composite material plate, *Composite Structure* (2003), 61, 27–38.
- [4] ASTM D3029. Standard test method for impact resistance of rigid plastic sheeting or parts by means of a tup (Falling Weight). American Society for Testing and Materials, 1982.
- [5] Allix O. and Feissel P., Modified constitutive relation error identification strategy for transient dynamics with corrupted data: The elastic case, *Comput. Methods* (2007), 196, 1968–1983.
- [6] Grolleau V., Gary G. and Mohr D., Biaxial Testing of Sheet Materials at High Strain Rates Using Viscoelastic Bars, (2007), 48, 293–306.
- [7] Zhao H., Elnasri I. and Girard Y., « Perforation of aluminium foam core sandwich panels under impact loading—An experimental study », *Intern. J. of Imp. Eng.*, (2007), 34, 1246–1257.
- [8] Hockauf M., Meyer LW., Pursche F. and Diestel O., Dynamic perforation and force measurement for lightweight materials by reverse ballistic impact, *Compos. Part A*, (2007), 38, 849–857.
- [9] Hild F. and Roux S. « Digital Image Correlation: From Displacement Measurement to Identification of Elastic Properties - A Review », *Strain*, (2006), 42, 69–80.